University of Manchester
Department of Physics and Astronomy
3rd Year Laboratory

An introduction to radio telescopes and pulsar astronomy

http://www.jb.man.ac.uk/research/pulsar/lab

1. OUTLINE

Note that this experiment requires a reasonable aptitude for programming in C or C++.

This experiment runs for four weeks. You will spend the Tuesday of each week carrying out experimental and observational work at Jodrell Bank and the Thursdays on carrying out data analysis and background reading in Manchester. The topics covered are as follows:

Week 1: An introduction to radio telescopes. You will measure the beam shape of the telescope by performing scans across a strong radio source. Using the 42-ft telescope you will make relative flux density measurements of some strong radio sources compared with a calibration noise source.

Weeks 2 & 3: An introduction to pulsar astronomy. You will use some existing data obtained with the 76-m Lovell radio telescope to search for the presence of a radio pulsar and to measure its period. To do this, you will write a programme and use simple Fourier analysis techniques. You will then use existing data obtained with the 42-ft telescope on the 'Crab pulsar' to measure pulse arrival times at the observatory over a period of a few days. These times must be corrected to the barycentre of the Solar System to obtain the true period and its first derivative. This entails writing a second computer program to analyse and correct the arrival time data. From the results the age and surface magnetic field of the neutron star in the Crab Nebula can be deduced.

Week 4: Determining the 'dispersion measure' of a pulsar. Using the 42-ft telescope you will measure pulse arrival times as a function of observing frequency and hence calculate the dispersion measure. You can then determine the approximate distance to the pulsar.

It is most important that you keep a careful running record of your observational and analytical work in your laboratory notebook. To complete the experiment properly, you will need to tackle all the problems set out in bold font in this script.

---

1 Background reading

Some suggestions for background reading:

- Background information about pulsars is given in the article by Lorimer "Radio Pulsars: An Observer's Perspective" and a more detailed review which both can be found online[1].
- See http://www.jb.man.ac.uk/research/pulsar/Education/
- Textbook "Handbook of Pulsar Astronomy" by Duncan Lorimer and Michael Kramer
- Textbook "Pulsar Astronomy" by Lyne & Graham-Smith

[1] Radio Pulsars: An Observer's Perspective: http://www.jb.man.ac.uk/research/pulsar/lab/lorimer99.pdf
Detailed review: http://relativity.livingreviews.org/Articles/lrr-2001-5

The primary reflecting surface of the telescope is a paraboloid of revolution which focusses the incoming radiation onto the 'feed' aerial (see Fig. 1). Its action is, therefore, to turn plane waves into spherical waves whose centre of curvature is at the primary focus. In order to maximise the efficiency of the telescope, power reflected from near the edges of the dish must be collected by the feed. However, in so doing unwanted power will also be picked up from the surroundings of the telescope; this is termed 'spillover'. The response of the feed as a function of direction is therefore tailored to maximise the ratio between the 'gain' of the telescope and the overall system noise temperature to which the spillover contributes (see below).

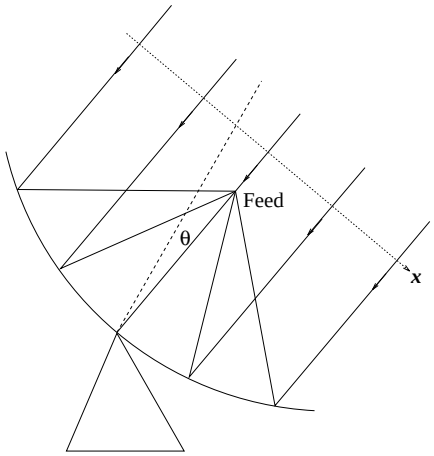

Figure 1: Schematic diagram of a radio telescope

2.1 The Beamshape and the Aperture Illumination

To understand the response of the telescope as a function of direction it may be easier to think about waves being transmitted from the feed and reflected off the paraboloid and into space; the telescope's characteristics are identical when transmitting or receiving (the reciprocity theorem). The waves from the feed excite changing currents in the reflecting surface and these in turn result in electromagnetic waves being radiated in the forward direction; the overall *far field* pattern of the telescope (its *voltage polar diagram*) is a combination of these plane waves. This is *Fraunhofer diffraction*. The *aperture distribution* $A(x)$ of surface currents is related to the voltage polar diagram, $P(\theta)$, by a Fourier Transform relationship. In one dimension:

$$P(\theta) = \int_{-D/2}^{D/2} A(x) e^{i(2\pi x/\lambda)\theta} \mathrm{d}x,$$

where D is the diameter of the telescope, and λ is the observing wavelength (consult Hecht 'Optics', Chapter 10).

An equivalent way to understand the 'Fourier pair' relationship between the aperture distribution and the far field pattern is to imagine the aperture distribution being made up from a set of sinusoidal standing waves (effectively a set of notional diffraction gratings across the aperture). By Fourier's Theorem any such spatial distribution can be constructed out of a weighted set of sinusoids (spatial Fourier components). Each sinusoidal diffraction grating of spatial wavelength d gives rise to two plane waves (at $\pm\theta$ where $\theta = \lambda/d$) and the integrated effect of the plane waves from all the spatial Fourier components in the aperture produces the voltage polar diagram. Note the inverse relation between θ and d which is characteristic of a Fourier pair – the smaller is the spatial dimension involved, the larger is the angle over which waves are radiated. The larger is the telescope diameter, the longer are the spatial Fourier components which can can be 'fitted in' to the aperture and hence the more power which is radiated at small angles.

N.B. Since the receiving system you are using responds to the total *power* rather than the complex voltage, the beam pattern you measure by scanning the telescope is called the *power polar diagram* of the telescope.

The Fourier transform of a disk, the geometrical shape of the aperture of the telescope, is called a first-order Bessel function and the square of this function, giving the power polar diagram, has a full-width at half maximum of $1.02\lambda/D$ radians, where D is the diameter of the telescope and λ is the wavelength.

Scan the telescope across the strong source Cass A (see Appendix A, but ask the lab demonstrator for some additional instructions first) and measure the width of the power polar diagram (power polar representation of the telescope beam) between half-power points. Is this consistent with the known diameter of the telescope? Can you explain any differences?

2.3 Calibration and Noise Temperature Measurements

Noise Temperature: Essentially all the signals we deal with in radio astronomy are pure random noise. The parameter most often used to characterise these signals is the 'noise temperature' T (measured in K) which is directly proportional to *mean noise power* available from a resistor at temperature T. From the theorem of equipartition of energy there are $kT/2$ Joules of energy associated with each 'degree of freedom' of the system, i.e. in each Hz and in each of the two polarisation states. Thus the power per unit bandwidth is kT Watts Hz^{-1} and over a bandwidth B Hz the total power available is kTB Watts. Absolute calibration measurements in radio astronomy are therefore made using 'hot and cold loads' which are resistors at well-defined temperatures (e.g. liquid He, liquid N and room temperature).

After amplification, the random noise signals, which have a zero mean, are turned into a more useful form by a *detector*. Usually in radio astronomy we use a device (most simply based on a diode operating on the bottom part of its characteristic curve) which responds to the square of the input voltage i.e. to the power of the random signal integrated over an appropriate period. In a basic receiver this period could be set by an RC 'time constant'. Because the statistical nature of the input signal there is a *random fluctuating* component in the detected signal (see Fig. 2) whose magnitude is $\propto T/\sqrt{B\tau}$ where τ is the time over which the signal is averaged. (Note that this is akin to the fluctuations $\propto \sqrt{N}$ in Poisson statistics). Thus the accuracy of the measurement of the mean power is increased by increasing the signal bandwidth and the averaging time.

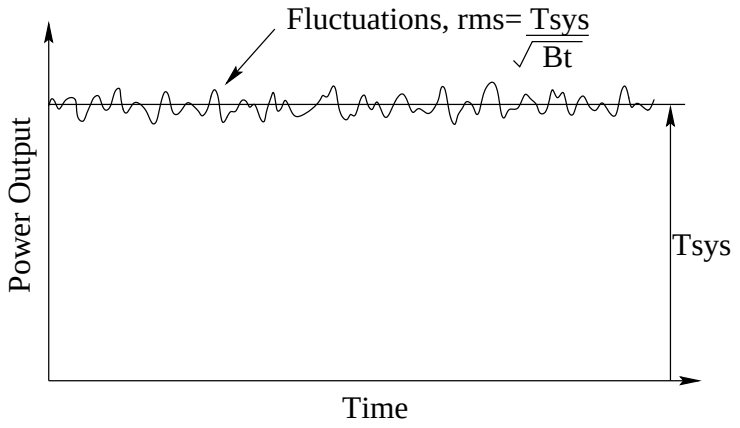

Figure 2: The noisy signal after square-law detection

The total noise power at the output of the receiver, often called the 'system noise temperature' $T_{\rm sys}$, has several contributions:

i) $T_{\rm source}$, the desired contribution coming from the radio source.

ii) $T_{\rm sky}$, the contribution from the sky around the source.

iii) $T_{\rm spillover}$, the contribution from the ground around the telescope.

iv) $T_{\rm rec}$, the noise generated in the receiver electronics.

Because we are dealing with random noise signals the powers add i.e.

$$T_{\rm sys} = T_{\rm source} + T_{\rm sky} + T_{\rm spillover} + T_{\rm rec}.$$

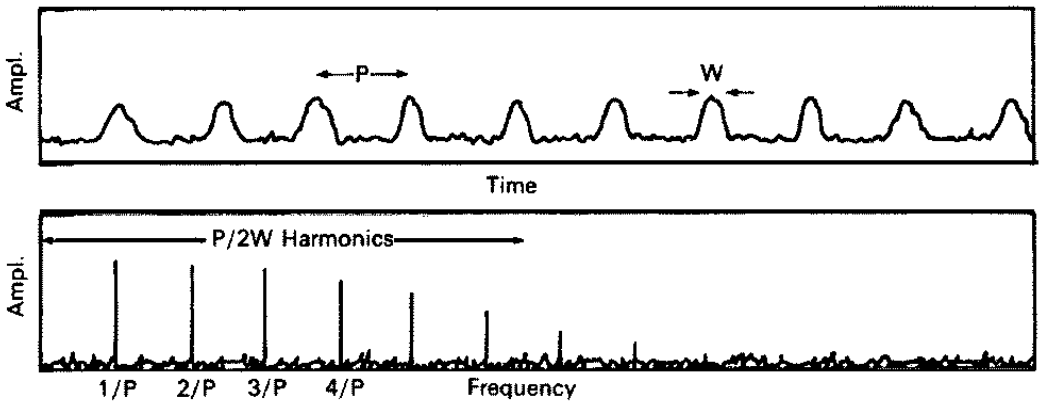

Figure 3: The spectrum of a sequence of pulses from a pulsar, taken from Fig. 3.3 of "Pulsar Astronomy" by Lyne and Smith (1998).

For these observations $T_{\rm sys} \approx 100$K, $T_{\rm sky} \approx 20$ K and $T_{\rm spillover} \approx 10$ K. The 'aperture efficiency' of the 42-ft telescope is $\sim 55\%$ (i.e its effective collecting area is 55% of its physical area). This translates to a sensitivity of 0.026 K Jy^{-1} and therefore if the source has a flux density of 100 Jy the noise contribution corresponds to 2.6 K. Note that 1 Jy corresponds to 10^{-26} W m^{-2} Hz^{-1} and that it is a measure of the power falling on unit area per unit bandwidth.

The flux density at 610 MHz of the calibration sources of interest to your observations are: Cassiopaeia A, 3595 Jy (epoch 1990, decreasing at 1.03 % per year) and Cygnus A, 3555 Jy. Their contributions to $T_{\rm sys}$ are therefore $\approx$ 93K and $\approx$ 92K respectively. These are the strongest sources in the sky; usually radio astronomers observe much weaker sources whose contribution is therefore $\ll T_{\rm sys}$.

If the signal bandwidth of your receiving system is 8 MHz, what averaging time must be used in order to detect a 1 Jy source with a signal-to-noise ratio of 10:1?

Scan the telescope across the radio sources Cass A and Cygnus A (provided they are above the horizon) and compare the deflection on the pen recorder (which measures the total power from the system) with that from the 'CAL' signal. Establish the magnitude of CAL in Jy. Make scans across one or both of Taurus A (the Crab Nebula) and Virgo A and use the calibration you have just derived to establish the flux density of these sources. Quote the errors on your answers.

---

3. AN INTRODUCTION TO PULSAR ASTRONOMY

Pulsars were discovered in 1967 by Bell & Hewish at Cambridge. Within a year it was accepted that they were rotating neutron stars. The 76-m Lovell telescope, as well as the 42-ft telescope, are more flexible instruments for studying known pulsars and for finding new ones than the dipole array used by Bell & Hewish. A significant part of the subsequent detective work on pulsars has therefore been carried out at Jodrell Bank.

3.1 Detection of an unknown pulsar and measurement of its period

One of the greatest challenges in pulsar astronomy is the discovery of pulsars of unknown periodicity. Only once the period is known can the pulsar data be "folded" to produce high signal-to-noise ratio profiles which can be used to study the pulsar in detail. This search process is now carried out by inspection of the power spectrum of the data which will show delta functions at the fundamental rotation frequency of the pulsar and its harmonics, the number of harmonics being roughly equal to $P/2W$, where P is pulse period and W is the pulse width (see figure 3). From the frequency of the Nth harmonic, $\nu_{\rm N}$,

the frequency of the fundamental and its error can be estimated as $(\nu_N \pm 0.5\Delta\nu)/N$, where $\Delta\nu$ is the frequency interval in the spectrum and equal to $1/T$, where T is the total duration of the time sequence. Thus the most accurate estimate of the frequency can be obtained from the highest clearly detectable harmonic.

Write a computer program to perform the Fourier transform of a time sequence of samples obtained with the 76-m Lovell radiotelescope (ask your lab demonstrator for a template for the computer code and data). By graphical inspection of the resultant amplitude spectrum (obtained by calculating the amplitude of each of the complex numbers in the spectrum), estimate the frequency and width of the pulses in the time sequence.

3.2 Pulse arrival times from the Crab pulsar

Much can be inferred about the physics of neutron stars and their binary companions (if present) from an analysis of the precise arrival times of the pulses. You will be supplied with a set of profiles obtained with the 42-ft telescope, on the powerful pulsar in the Crab Nebula. The data were taken by folding the data using an approximate period, on two separate days with a gap of several days between them. Before one can use these data for physical interpretation they must be corrected for the motion of the observatory around the Sun, i.e. the pulse train should appear to have been collected at a fixed point in space. The most convenient point to use is the centre of mass of the Solar System, its *barycentre*.

Data on the position of the centre of the Earth with respect to the barycentre are given in the *Astronomical Almanac* and will be provided by the lab demonstrator. However, since positions are only given once per day, it is necessary to interpolate between the data points to be able to correct the arrival times to a sufficient precision. The typical error in the arrival time of a pulse in the raw data is ~ 0.2 milliseconds, and the interpolation error must be less than this. An additional correction is required because the observatory is not located at the centre of the Earth! It has a very simple form: $r\sin(\epsilon)/c$, where r is the radius of the Earth, ϵ is the elevation of the source above the horizon and c is the velocity of light. **Justify the form of this correction with a simple diagram.** The actual elevation of the pulsar is given for each profile in the data set with which you are supplied.

Draw a diagram which demonstrates the principles of the barycentric correction. Write a computer program to perform the interpolation between the barycentre positions supplied by the lab demonstrator using one of the Lagrange multi-point formulas (see Appendix C) after determining which one is suitable. Determine the light travel times from the Earth's centre to the Solar System barycentre. Make the further correction dependent on the elevation of the pulsar.

It is straightforward to determine the raw arrival times (defined as the time the pulse arrives after the beginning of the scan) from the data provided by the lab demonstrator. These data are the input data to a computer program which determines an accurate period for the individual days. The philosophy behind your program can be as follows:

By definition any two arrival times should be separated by an integer number of pulse periods. However, if the current estimate of the pulse period is incorrect, dividing the time separation by the period will not produce an integer. Provided the estimate is not far wrong, taking the nearest integer and dividing the separation by this integer will yield a more accurate estimate of the pulse period. Ask the lab demonstrator for an initial estimate for the period of the Crab pulsar. This value is accurate enough to obtain the correct integer number of periods over a 10-min interval. Use the current period estimate to calculate arrival times throughout the day and subtract these from the raw data. These 'residuals' will systematically grow throughout the day. Plot the residuals against time and use the slope (determined by least-squares fitting) to make a better estimate of the pulse period. By iterating around this loop it should be possible to eliminate systematic trends in the plot of residuals and hence to arrive at the best estimate of the period for that day.

Write a computer program to determine an accurate pulse period for each of the two days; include the barycentric correction program as a subroutine. Determine the period derivative and hence estimate the age of the pulsar and its surface magnetic field. Quote the errors on your answers.

3.3 Measurement of pulsar dispersion measures

On its way to the Earth the pulsed radiation passes through ionised plasma in the interstellar medium (ISM). The refractive index of plasma is a function of frequency and hence the radiation experiences a frequency dependent delay – i.e. the ISM is dispersive. From the difference in arrival time as a function of frequency one can calculate the 'dispersion measure', the integrated electron number density along the line-of-sight to the pulsar i.e.

$$DM = \int_{\text{pulsar}}^{\text{earth}} n_e \cdot \mathrm{d}l.$$

More details about the frequency dispersion in pulse arrival time are given in Appendix D. The dispersive effect of the ISM causes initially sharp pulses to become smeared in addition to suffering an overall delay, when observed with a receiver with a finite bandwidth. This pulse-smearing effect must be removed by special-purpose electronics ('de-dispersers') in order to restore the original signal-to-noise ratio.

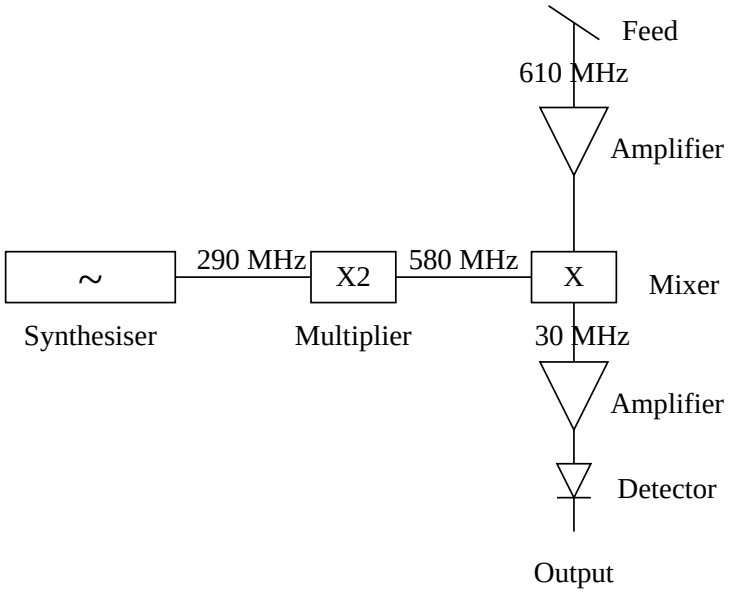

Figure 4: Schematic diagram of the heterodyne receiver

The receiver on the 42-ft telescope is a heterodyne one. The noise signals collected by the telescope are 'mixed' with a pure sinusoidal local oscillator (LO) signal. The difference signals are lower frequencies which are more convenient for filtering and amplification and passing along long lengths of cable from the focus box to the observing room. A simplified diagram of your receiver is shown in Fig. 4. The LO signal is generated in a frequency synthesiser whose output frequency can be changed at will. Note that the synthesiser signal for the first LO is doubled in a non-linear 'multiplier'.

Measure the change in arrival time of pulses as a function of frequency from observations at ≥ 3 frequencies (ask the lab demonstrator for instructions). Use the relevant equation in Appendix D to determine the dispersion measure of the pulsar. Assuming a value of the mean electron density in the ISM of 0.03 cm^{-3} calculate the distance of the pulsar. Compare your value with the published value.

Appendix A: Making scans with the 42-ft telescope

The 42-ft telescope is controlled with a computer called ARTHUR. After consulting the lab demonstrator, the following procedure should be followed to make a scan:

1. The 42-ft telescope is used most of the time for scientific pulsar observations, so it is important to stop those observations first before you start. This is done in the program called menu2 (NEVER RUN menu INSTEAD OF menu2!). Commands are entered by pressing the "DO" key, which you can find on the keyboard. Enter the commands "abort" and "close". Use the '-' key on the numeric keypad to go back in a menu.

2. The telescope is controlled via the program "telc", which will ask which telescope you want to opperate. Type "42ft" and you see the time (UT and ST), the pointing position (actual and demanded), the requested coordinates, source offset and offset rates. To move to for instance CAS A press the DO key and type its coordinates: "2000 23:23:26.4 58:49:34.0", where the 2000 means you entered the coordinates with respect to epoch 2000. To scan over the source you can press the DO-key and type "offset 5 0" to start with an azimuth offset of 5° (and an elevation offset of 0°). Then enter the command "offrate -2.5 0" to scan back in azimuth with 2.5 deg/min. When the scan is completed you can stop scanning by entering the commande "offrate 0 0".

3. You will record the signal using a chart recorder. A speed of 30mm/min should give a good plot. DO NOT WASTE PAPER, so stop the recorder if you are not recording useful data and do not use excessive speeds. MAKE NOTES IN YOUR LABSCRIPT OR ON THE CHART WHAT SPEED SETTING WAS USED FOR WHICH CHART! Most likely you should adjust the offset and scale settings on the chart recorder to get a good plot.

25. Numerical Interpolation, Differentiation, and Integration

Numerical analysts have a tendency to accumulate a multiplicity of tools each designed for highly specialized operations and each requiring special knowledge to use properly. From the vast stock of formulas available we have culled the present selection. We hope that it will be useful. As with all such compendia, the reader may miss his favorites and find others whose utility he thinks is marginal.

We would have liked to give examples to illuminate the formulas, but this has not been feasible. Numerical analysis is partially a science and partially an art, and short of writing a textbook on the subject it has been impossible to indicate where and under what circumstances the various formulas are useful or accurate, or to elucidate the numerical difficulties to which one might be led by uncritical use. The formulas are therefore issued together with a caveat against their blind application.

Formulas

Notation: Abscissas: $x_0<x_1<\ldots$; functions: $f, g, \ldots$; values: $f(x_i)=f_i, f'(x_i)=f_i'$. $f', f^{(2)}, \ldots$ indicate 1st, 2d, ... derivatives. If abscissas are equally spaced, $x_{i+1}-x_i=h$ and $f_p=f(x_0+ph)$ (p not necessarily integral). R, R_n indicate remainders.

25.1. Differences

Forward Differences

25.1.1

$$\Delta(f_n)=\Delta_n=\Delta_n^1=f_{n+1}-f_n$$

$$\Delta_n^2=\Delta_{n+1}^1-\Delta_n^1=f_{n+2}-2f_{n+1}+f_n$$

$$\Delta_n^3=\Delta_{n+1}^2-\Delta_n^2=f_{n+3}-3f_{n+2}+3f_{n+1}-f_n$$

$$\Delta_n^k=\Delta_{n+1}^{k-1}-\Delta_n^{k-1}=\sum_{j=0}^{k}(-1)^j\binom{k}{j}f_{n+k-j}$$

Central Differences

25.1.2

$$\delta(f_{n+\frac12})=\delta_{n+\frac12}=\delta_{n+\frac12}^1=f_{n+1}-f_n$$

$$\delta_n^2=\delta_{n+\frac12}^1-\delta_{n-\frac12}^1=f_{n+1}-2f_n+f_{n-1}$$

$$\delta_{n+\frac12}^3=\delta_{n+1}^2-\delta_n^2=f_{n+2}-3f_{n+1}+3f_n-f_{n-1}$$

$$\delta_n^{2k}=\sum_{j=0}^{2k}(-1)^j\binom{2k}{j}f_{n+k-j}$$

$$\delta_{n+\frac12}^{2k+1}=\sum_{j=0}^{2k+1}(-1)^j\binom{2k+1}{j}f_{n+k+1-j}$$

$\delta_{\frac12 n}^k=\Delta_{\frac12(n-k)}^k$ if n and k are of same parity.

Forward Differences

x_0	f_0			
		Δ_0		
x_1	f_1		Δ_0^2	
		Δ_1		Δ_0^3
x_2	f_2		Δ_1^2	
		Δ_2		
x_3	f_3			

Central Differences

x_{-1}	f_{-1}			
		$\delta_{-\frac12}$		
x_0	f_0		δ_0^2	
		$\delta_{\frac12}$		$\delta_{\frac12}^3$
x_1	f_1		δ_1^2	
		$\delta_{3/2}$		
x_2	f_2			

Mean Differences

25.1.3

$$\mu(f_n)=\tfrac12(f_{n+\frac12}+f_{n-\frac12})$$

Divided Differences

25.1.4

$$[x_0,x_1]=\frac{f_0-f_1}{x_0-x_1}=[x_1,x_0]$$

$$[x_0,x_1,x_2]=\frac{[x_0,x_1]-[x_1,x_2]}{x_0-x_2}$$

$$[x_0,x_1,\ldots,x_k]=\frac{[x_0,\ldots,x_{k-1}]-[x_1,\ldots,x_k]}{x_0-x_k}$$

Divided Differences in Terms of Functional Values

25.1.5

$$[x_0,x_1,\ldots,x_n]=\sum_{k=0}^{n}\frac{f_k}{\pi_n'(x_k)}$$

25.1.6 where $\pi_n(x)=(x-x_0)\ (x-x_1)\ \ldots\ (x-x_n)$ and $\pi_n'(x)$ is its derivative:

25.1.7

$$\pi_n'(x_k)=(x_k-x_0)\ \ldots\ (x_k-x_{k-1})(x_k-x_{k+1})\ \ldots\ (x_k-x_n)$$

Let D be a simply connected domain with a piecewise smooth boundary C and contain the points $z_0, \ldots, z_n$ in its interior. Let $f(z)$ be analytic in D and continuous in $D+C$. Then,

25.1.8

$$[z_0,z_1,\ldots,z_n]=\frac{1}{2\pi i}\int_C\frac{f(z)}{\prod_{k=0}^{n}(z-z_k)}\,dz$$

25.1.9

$$\Delta_0^n=h^nf^{(n)}(\xi)\qquad(x_0<\xi<x_n)$$

25.1.10

$$[x_0,x_1,\ldots,x_n]=\frac{\Delta_0^n}{n!h^n}=\frac{f^{(n)}(\xi)}{n!}\qquad(x_0<\xi<x_n)$$

25.1.11

$$[x_{-n},x_{-n+1},\ldots,x_0,\ldots,x_n]=\frac{\delta_0^{2n}}{h^{2n}(2n)!}$$

Reciprocal Differences

25.1.12

$$\rho(x_0,x_1)=\frac{x_0-x_1}{f_0-f_1}$$

$$\rho_2(x_0,x_1,x_2)=\frac{x_0-x_2}{\rho(x_0,x_1)-\rho(x_1,x_2)}+f_1$$

$$\rho_3(x_0,x_1,x_2,x_3)=\frac{x_0-x_3}{\rho_2(x_0,x_1,x_2)-\rho_2(x_1,x_2,x_3)}+\rho(x_1,x_2)$$

$$\rho_n(x_0,x_1,\ldots,x_n)=\frac{x_0-x_n}{\rho_{n-1}(x_0,\ldots,x_{n-1})-\rho_{n-1}(x_1,\ldots,x_n)}+\rho_{n-2}(x_1,\ldots,x_{n-1})$$

25.2. Interpolation

Lagrange Interpolation Formulas

25.2.1

$$f(x)=\sum_{i=0}^{n}l_i(x)f_i+R_n(x)$$

25.2.2

$$l_i(x)=\frac{\pi_n(x)}{(x-x_i)\pi_n'(x_i)}=\frac{(x-x_0)\ \ldots\ (x-x_{i-1})(x-x_{i+1})\ \ldots\ (x-x_n)}{(x_i-x_0)\ \ldots\ (x_i-x_{i-1})(x_i-x_{i+1})\ \ldots\ (x_i-x_n)}$$

Remainder in Lagrange Interpolation Formula

25.2.3

$$R_n(x)=\pi_n(x)\cdot[x_0,x_1,\ldots,x_n,x]=\pi_n(x)\cdot\frac{f^{n+1}(\xi)}{(n+1)!}\qquad(x_0<\xi<x_n)$$

25.2.4

$$|R_n(x)|\le\frac{(x_n-x_0)^{n+1}}{(n+1)!}\max_{x_0\le x\le x_n}|f^{(n+1)}(x)|$$

25.2.5

$$R_n(z)=\frac{\pi_n(z)}{2\pi i}\int_C\frac{f(t)}{(t-z)(t-z_0)\ldots(t-z_n)}\,dt$$

The conditions of **25.1.8** are assumed here.

Lagrange Interpolation, Equally Spaced Abscissas

n Point Formula

25.2.6

$$f(x_0+ph)=\sum_k A_k^n(p)f_k+R_{n-1}$$

For n even, $\left(-\frac12(n-2)\le k\le\frac12 n\right)$.

For n odd, $\left(-\frac12(n-1)\le k\le\frac12(n-1)\right)$.

25.2.7

$$A_k^n(p)=\frac{(-1)^{\frac12 n+k}}{\left(\frac{n-2}{2}+k\right)!\,(\frac12 n-k)!\,(p-k)}\prod_{t=1}^{n}(p+\tfrac12 n-t)\qquad n\text{ even.}$$

$$A_k^n(p)=\frac{(-1)^{\frac12(n-1)+k}}{\left(\frac{n-1}{2}+k\right)!\left(\frac{n-1}{2}-k\right)!\,(p-k)}\prod_{t=0}^{n-1}\left(p+\frac{n-1}{2}-t\right),\qquad n\text{ odd.}$$

25.2.8

$$R_{n-1}=\frac{1}{n!}\prod_k(p-k)h^nf^{(n)}(\xi)\approx\frac{1}{n!}\prod_k(p-k)\Delta_0^n\qquad(x_0<\xi<x_n)$$

k has the same range as in **25.2.6.**

Lagrange Two Point Interpolation Formula (Linear Interpolation)

25.2.9

$$f(x_0+ph)=(1-p)f_0+pf_1+R_1$$

25.2.10

$$R_1(p)\approx.125h^2f^{(2)}(\xi)\approx.125\Delta^2$$

Lagrange Three Point Interpolation Formula

25.2.11

$$f(x_0+ph)=A_{-1}f_{-1}+A_0f_0+A_1f_1+R_2$$
$$\approx\frac{p(p-1)}{2}f_{-1}+(1-p^2)f_0+\frac{p(p+1)}{2}f_1$$

25.2.12

$$R_2(p)\approx .065h^3f^{(3)}(\xi)\approx .065\Delta^3 \qquad (|p|\leq 1)$$

Lagrange Four Point Interpolation Formula

25.2.13

$$f(x_0+ph)=A_{-1}f_{-1}+A_0f_0+A_1f_1+A_2f_2+R_3$$
$$\approx\frac{-p(p-1)(p-2)}{6}f_{-1}+\frac{(p^2-1)(p-2)}{2}f_0$$
$$-\frac{p(p+1)(p-2)}{2}f_1+\frac{p(p^2-1)}{6}f_2$$

25.2.14 $R_3(p)\approx$

$.024h^4f^{(4)}(\xi)\approx .024\Delta^4$ $(0<p<1)$

$.042h^4f^{(4)}(\xi)\approx .042\Delta^4$ $(-1<p<0,\ 1<p<2)$

$(x_{-1}<\xi<x_2)$

Lagrange Five Point Interpolation Formula

25.2.15

$$f(x_0+ph)=\sum_{i=-2}^{2}A_if_i+R_4$$
$$\approx\frac{(p^2-1)p(p-2)}{24}f_{-2}-\frac{(p-1)p(p^2-4)}{6}f_{-1}$$
$$+\frac{(p^2-1)(p^2-4)}{4}f_0-\frac{(p+1)p(p^2-4)}{6}f_1$$
$$+\frac{(p^2-1)p(p+2)}{24}f_2$$

25.2.16 $R_4(p)\approx$

$.012h^5f^{(5)}(\xi)\approx .012\Delta^5$ $(|p|<1)$

$.031h^5f^{(5)}(\xi)\approx .031\Delta^5$ $(1<|p|<2)$ $(x_{-2}<\xi<x_2)$

Lagrange Six Point Interpolation Formula

25.2.17

$$f(x_0+ph)=\sum_{i=-2}^{3}A_if_i+R_5$$
$$\approx\frac{-p(p^2-1)(p-2)(p-3)}{120}f_{-2}$$
$$+\frac{p(p-1)(p^2-4)(p-3)}{24}f_{-1}$$
$$-\frac{(p^2-1)(p^2-4)(p-3)}{12}f_0$$
$$+\frac{p(p+1)(p^2-4)(p-3)}{12}f_1-\frac{p(p^2-1)(p+2)(p-3)}{24}f_2$$
$$+\frac{p(p^2-1)(p^2-4)}{120}f_3$$

25.2.18 $R_5(p)\approx$

$.0049h^6f^{(6)}(\xi)\approx .0049\Delta^6$ $(0<p<1)$

$.0071h^6f^{(6)}(\xi)\approx .0071\Delta^6$ $(-1<p<0,\ 1<p<2)$

$.024h^6f^{(6)}(\xi)\approx .024\Delta^6$ $(-2<p<-1,\ 2<p<3)$

$(x_{-2}<\xi<x_3)$

Lagrange Seven Point Interpolation Formula

25.2.19

$$f(x_0+ph)=\sum_{i=-3}^{3}A_if_i+R_6$$

25.2.20

$$R_6(p)\approx\begin{cases}.0025h^7f^{(7)}(\xi)\approx .0025\Delta^7 & (|p|<1)\\ .0046h^7f^{(7)}(\xi)\approx .0046\Delta^7 & (1<|p|<2)\\ .019h^7f^{(7)}(\xi)\approx .019\Delta^7 & (2<|p|<3)\end{cases}$$

$(x_{-3}<\xi<x_3)$

Lagrange Eight Point Interpolation Formula

25.2.21

$$f(x_0+ph)=\sum_{i=-3}^{4}A_if_i+R_7$$

25.2.22

$$R_7(p)\approx\begin{cases}.0011h^8f^{(8)}(\xi)\approx .0011\Delta^8 & (0<p<1)\\ .0014h^8f^{(8)}(\xi)\approx .0014\Delta^8 & (-1<p<0)\ (1<p<2)\\ .0033h^8f^{(8)}(\xi)\approx .0033\Delta^8 & (-2<p<-1)\ (2<p<3)\\ .016h^8f^{(8)}(\xi)\approx .016\Delta^8 & (-3<p<-2)\ (3<p<4)\end{cases}$$

$(x_{-3}<\xi<x_4)$

Aitken's Iteration Method

Let $f(x|x_0, x_1, \ldots, x_k)$ denote the unique polynomial of k^{th} degree which coincides in value with $f(x)$ at $x_0, \ldots, x_k$.

25.2.23

$$f(x|x_0,x_1)=\frac{1}{x_1-x_0}\begin{vmatrix}f_0 & x_0-x\\ f_1 & x_1-x\end{vmatrix}$$

$$f(x|x_0,x_2)=\frac{1}{x_2-x_0}\begin{vmatrix}f_0 & x_0-x\\ f_2 & x_2-x\end{vmatrix}$$

$$f(x|x_0,x_1,x_2)=\frac{1}{x_2-x_1}\begin{vmatrix}f(x|x_0,x_1) & x_1-x\\ f(x|x_0,x_2) & x_2-x\end{vmatrix}$$

$$f(x|x_0,x_1,x_2,x_3)=\frac{1}{x_3-x_2}\begin{vmatrix}f(x|x_0,x_1,x_2) & x_2-x\\ f(x|x_0,x_1,x_3) & x_3-x\end{vmatrix}$$

Reaching such a small fraction of the receiver noise level is commonly achieved in radio astronomical observations by using a wide receiver bandwidth B and averaging the signal over an integration time τ. The smallest detectable signal is then a fraction $(B\tau)^{-1/2}$ of the total noise level. Typically, a receiver might have a bandwidth of 1 MHz, and it may be required to detect a single pulse 10 milliseconds long; the sensitivity would then be 10^{-2} of the input noise, or about 1 Jy in a large radio telescope. Single pulses are rarely as strong as 1 Jy, and weaker pulses would be lost in noise. However a series of 10 000 pulses, suitably added together, would provide a further factor of 10^{-2}, giving a more useful sensitivity of 10^{-2} Jy within the averaged pulse; the mean flux density of a detectable pulsar will, of course, be lower than this, depending on the ratio of pulse width to period.

3.2 Frequency dispersion in pulse arrival time

Although the basic characteristic of the pulsar signal which facilitates its recognition is the precise periodicity, a second important characteristic is the frequency dispersion in arrival time due to the ionised interstellar medium. This may assist the recognition of a pulsar signal against locally generated impulsive radio interference, but it also plays an important part in restricting the range of a pulsar search.

Radio pulses travel in the ionised interstellar medium at the group velocity v_g, which for small electron densities is related to the free space velocity c by

$$v_g \simeq c\left(1 - \frac{n_e e^2 \lambda^2}{2\pi m c^2}\right) = c\left(1 - \frac{n_e e^2}{2\pi m \nu^2}\right) \tag{3.1}$$

where n_e is the electron number density and e and m are the electronic charge and mass. Hence the travel time T over distance L is

$$T = \int_0^L \frac{dl}{v_g} \simeq \frac{L}{c} + \frac{e^2 \int_0^L n_e dl}{2\pi m c \nu^2} = \frac{L}{c} + 1.345 \times 10^{-3} \nu^{-2} \int_0^L n_e dl \text{ s.} \tag{3.2}$$

The first term here is just the free space travel time and the second is the additional dispersive delay t. Customary units in astrophysics are parsecs (3×10^{18} cm) for distance and cm^{-3} for density: the integral $\int_0^L n_e dl$, which measures the total electron content between the pulsar and the observer, is known as dispersion measure, DM, with units cm^{-3} pc. Observers usually quote radio frequencies in megahertz, so that the delay t becomes

$$t = \frac{\text{DM}}{2.410 \times 10^{-4} \nu_{\text{MHz}}^2} \text{ s.} \tag{3.3}$$

The frequency dependence of this delay has a very important effect on observations of radio pulses. A short broad-band pulse will arrive earlier at higher frequencies, traversing the radio spectrum at a rate

$$\dot{\nu} = -1.205 \times 10^{-4} \frac{\nu_{\text{MHz}}^3}{\text{DM}} \text{ MHz s}^{-1}; \tag{3.4}$$

correspondingly, a receiver with bandwidth B (MHz) will stretch out a short pulse to

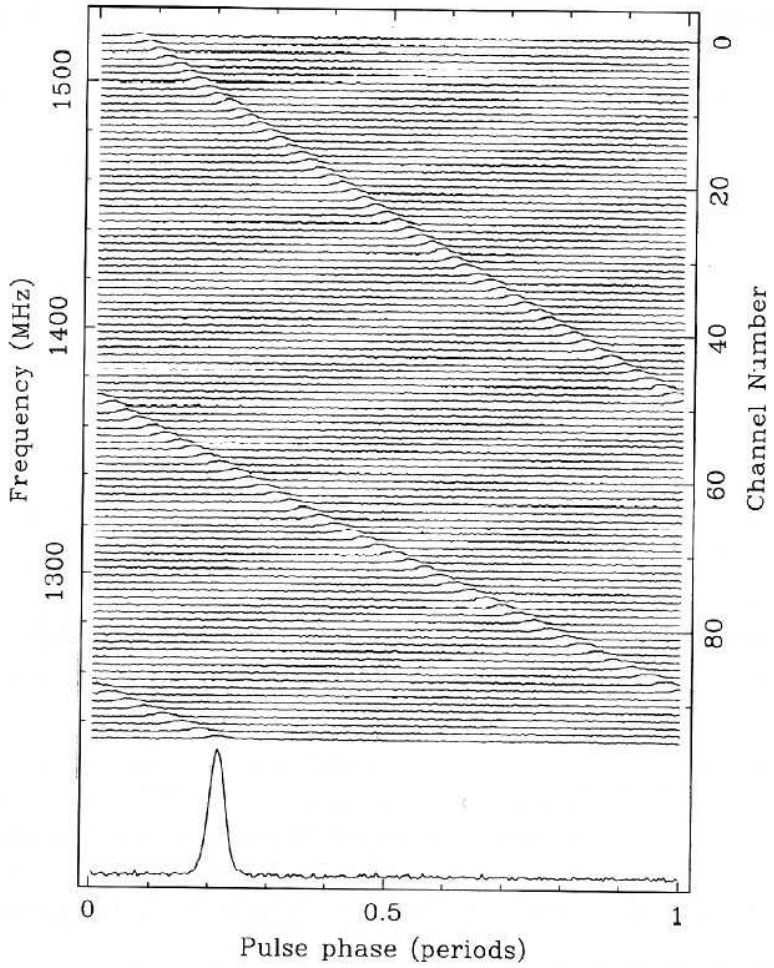

Fig. 3.1. Frequency dispersion in pulse arrival time for PSR B1641−45, recorded in 96 adjacent frequency channels, each 3 MHz wide, centred on 1380 MHz.

a length

$$\Delta t = 8.3 \times 10^3 \mathrm{DM} \nu_{\mathrm{MHz}}^{-3} B \text{ s}. \tag{3.5}$$

As a useful guide, $\Delta t = (202/\nu_{\mathrm{MHz}})^3$ DM milliseconds per MHz bandwidth.

If a pulsar with high dispersion measure is observed with a receiver with a wide bandwidth, its pulse is stretched and the peak intensity is reduced. The lost sensitivity may, however, be recovered by dividing a wide receiver bandwidth into separate bands and using separate receiver channels on each as in Figure 3.1. The output of these separate channels can then be added with appropriate delays so that the pulse components are properly superposed. This process of 'de-dispersion' is shown in Figure 3.2.

The technique first used for 'de-dispersion' involved a mechanically-driven sequential sampling of the separate receiver outputs (Large & Vaughan 1971). Digital techniques are now universally in use, either setting the individual delays to match the known DM of a given pulsar, or using a series of different delays in an off-line search through recorded data. Each set of delays then allows the detection of pulsars in a definite range of DM.

Andrew Lyne and Peter Wilkinson, with modifications from Dunc Lorimer, Patrick Weltevrede, Ben Stappers & Chris Jordan.

Last modified: September 2013